JACS
JOURNAL OF THE AMERICAN CHEMICAL SOCIETY

Communication

pubs.acs.org/JACS

An Azine-Linked Covalent Organic Framework

Sasanka Dalapati, Shangbin Jin, Jia Gao, Yanhong Xu, Atsushi Nagai, and Donglin Jiang*

Department of Materials Molecular Science, Institute for Molecular Science, National Institutes of Natural Sciences, 5-1 Higashiyama, Myodaiji, Okazaki 444-8787, Japan

Supporting Information

ABSTRACT: Condensation of hydrazine with 1,3,6,8-tetrakis(4-formylphenyl)pyrene under solvothermal conditions yields highly crystalline two-dimensional covalent organic frameworks. The pyrene units occupy the vertices and the diazabutadiene (−C═N−N═C−) linkers locate the edges of rohmbic-shaped polygon sheets, which further stack in an AA-stacking mode to constitute periodically ordered pyrene columns and one-dimensional microporous channels. The azine-linked frameworks feature permanent porosity with high surface area and exhibit outstanding chemical stability. By virtue of the pyrene columnar ordering, the azine-linked frameworks are highly luminescent, whereas the azine units serve as open docking sites for hydrogen-bonding interactions. These synergestic functions of the vertices and edge units endow the azine-linked pyrene frameworks with extremely high sensitivity and selectivity in chemosensing, for example, the selective detection of 2,4,6-trinitrophenol explosive. We anticipate that the extension of the present azine-linked strategy would not only increase the structural diversity but also expand the scope of functions based on this highly stable class of covalent organic frameworks.

Covalent organic frameworks (COFs) are a class of crystalline porous materials composed of lightweight elements and linked by covalent bonds, featuring precise periodicity in skeleton and predesignable pore parameter.[1] To discover new covalent bonds for the construction of such crystalline and permanent porous organic frameworks remains challenging in the field of reticular chemistry. Successful attempts to achieve COFs have been limited to few covalent bonds, including boronate,[2−10] boroxine,[2,11] borosilicate,[12] imine,[13,14] triazine,[15] hydrazone,[16] squaraine,[17] and borazine[18] linkages. Among them, only few examples of COFs have been reported to show enough high thermal and chemical stabilities, which however, are crucial for applications.[19] In this context, to explore a robust linkage for the synthesis of COFs that meet the requirement in crystallinity, porosity, and stability is of critical importance for the further advancement of the field from the viewpoints of both basic research and application.

Herein, we report the development of a new covalent bond based on the azine linkage for the synthesis of COFs that exhibit high crystallinity, high porosity, and robust chemical stability (Chart1, Py-Azine COF). Condensation of hydrazine with aldehydes is a thermodynamically controlled reaction that leads to the formation of azine derivatives and water byproducts. We utilized 1,3,6,8-tetrakis(4-formylphenyl)pyrene (Chart1, TFPPy) with four aldehyde groups at periphery as the aldehyde component to condense with hydrazine, with an aim to demonstrate the feasibility of the strategy and features of the new class of COFs. We found that the condensation under solvothermal conditions easily generated highly crystalline azine-linked pyrene COFs, which possess high porosity and robust stability. Especially the chemical stability of azine-linked COF is remarkable because they retain the crystalline structure upon keeping in polar and nonpolar organic solvents and even in inorganic acid and base such as aqueous HCl and NaOH solutions. Structural resolution based on X-ray diffraction measurement in conjunction with structural simulation indicates that Py-Azine COF consists of AA stacking structure, whereas the pyrene units at the vertices and the azine linkers on the edges of two-dimensional (2D) polygon sheets stack to form periodic pyrene columns and one-dimensional channels with open azine units on the pore walls. As a result, the COF is highly luminescent, whereas the azine sites serve as docking sites to lock guest molecules.[20] We highlight that the synergistic functions of vertices and edges endow the COF with unique chemosensing characteristics. As demonstrated in the vapor detection of 2,4,6-trinitrophenol explosive, the COF exhibits

Chart 1. (A) Schematic Representation of the Synthesis of the Azine-Linked COF (Py-Azine COF); (B) Top and Side Views of the AA Stacking Structure of the Py-Azine COF[a]

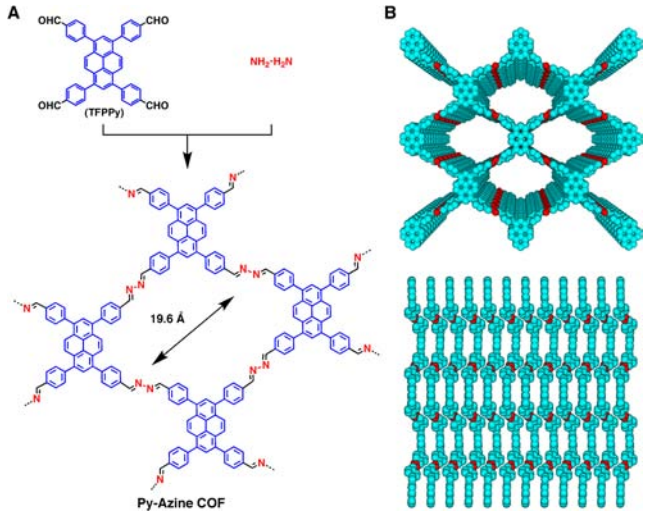

[a]Sky blue, tetraphenylpyrene unit; red, nitrogen; H atoms are omitted.

Received: October 8, 2013
Published: November 1, 2013

 © 2013 American Chemical Society dx.doi.org/10.1021/ja4103293 | J. Am. Chem. Soc. 2013, 135, 17310−17313

high sensitivity and selectivity. Exploration of COFs as chemosensing probes is unprecedented.

We screened the reaction conditions including the solvent, catalyst concentration, reaction temperature, and reaction time, for the condensation of TFPPy with hydrazine (Chart1). As for the solvent, one significant feature is that a variety of solvents can lead to the generation of crystalline frameworks (Figure S1, Supporting Information, SI). For example, solvents such as *o*-dichlorobenzene (*o*-DCB), *o*-DCB/*n*-BuOH (1.9/0.1 by vol), mesitylene/dioxane (1/3 by vol), and *o*-DCB/dioxane (3/1 by vol) in the presence of AcOH catalyst (6 M) give rise to crystalline polymers (Table S1). Among the solvents, reaction in *o*-DCB produced the COF with the highest X-ray diffraction (XRD) intensity, while the Brunauer–Emmett–Teller (BET) surface area is 599 $m^2\ g^{-1}$ (Table S1). The mixture of *o*-DCB/*n*-BuOH (1.9/0.1 by vol) yields crystalline Py-Azine COF that retains high XRD intensity and possesses the highest BET surface area of 1210 $m^2\ g^{-1}$. Decreasing the catalyst concentration causes the decrement of XRD intensity. A low reaction temperature such as 85 °C gives rise to low crystallinity. As an optimal condition, the Py-Azine COF was synthesized upon condensation of hydrazine with TFPPy under solvothermal condition in *o*-DCB/*n*-BuOH mixture (1.9/0.1, by vol) in the presence of AcOH catalyst (6 M, *o*-DCB/AcOH = 1.9/0.2 by vol) at 120 °C for 7 days, and isolated as pale yellow solid in 75% yield. Similarly, the model compound (Scheme S1) was synthesized as bright yellow powder in 99% yield.

Fourier-transform infrared (FT IR) spectroscopy of the Py-Azine COF exhibited a stretching vibration band at 1622 cm^{-1} assignable to the C═N bond (Figure S2). The model compound also displayed the C═N vibration band at 1622 cm^{-1}. Elemental analysis of the Py-Azine COF corroborates well with the theoretical values of infinite 2D sheet (SI). Field-emission scanning electron microscopy (FE-SEM) revealed that the Py-Azine COF adopts micrometer-scale belt morphology (Figure S3). Thermal gravimetric analysis (TGA) revealed that the Py-Azine COF is stable up to 250 °C (Figure S4).

The crystalline structure of the Py-Azine COF was resolved by the XRD measurements in conjunction with structural simulations. The Py-Azine COF exhibited strong XRD peaks at 4.48, 6.08, 9.0, 13.59, and 23.64°, which can be assigned to the 110, 200, 220, 330, and 001 facets, respectively (Figure 1A, red curve). The AA stacking mode (Figure 1B) can reproduce the peak position and intensity of the XRD pattern (Figure 1A, blue curve), whereas the AB stacking mode (Figure 1C) gives an XRD pattern (orange curve) that largely deviates from the experimentally observed profile. The Pawley refinement yielded an XRD pattern (Figure 1A, green curve) that is in good agreement with the experimentally observed pattern, as evident by their negligible difference (black curve). A monoclinic unit cell (C_2/m) with the parameters of a = 28.1415 Å, b = 28.8877 Å, c = 3.9107 Å, $\alpha = \gamma = 90°$, and β = 70.46° (SI) was deduced.

The porosity of the azine-linked COF was investigated by using the nitrogen sorption measurement at 77 K. As shown in Figure 2A, the sorption curve of the Py-Azine COF is classified as typical type I isotherm, which is characteristic of micro-porous polymers. The BET surface area and pore volume were estimated to be 1210 $m^2\ g^{-1}$ and 0.72 $cm^3\ g^{-1}$, respectively. The pore size distribution was evaluated by using the nonlocal density functional theory method resulted in a pore size centered at 1.76 nm, slightly tailing to the mesoporous region

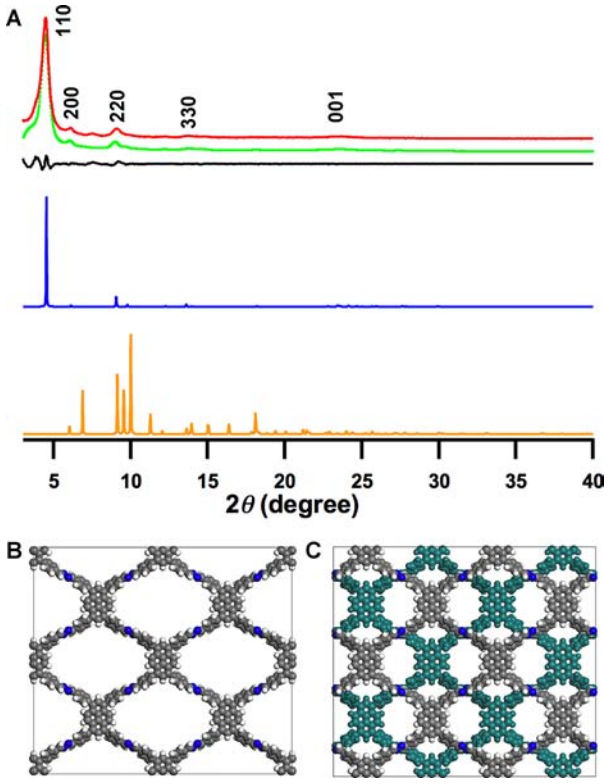

Figure 1. (A) XRD patterns of the Py-Azine COF: experimental (red), Pawley refined (green dotted line) difference between experimental and calculated data (black), calculated for AA-stacking (blue), and calculated for AB-stacking (orange). Space filling models of the Py-Azine COF in (B) AA and (C) AB stacking modes.

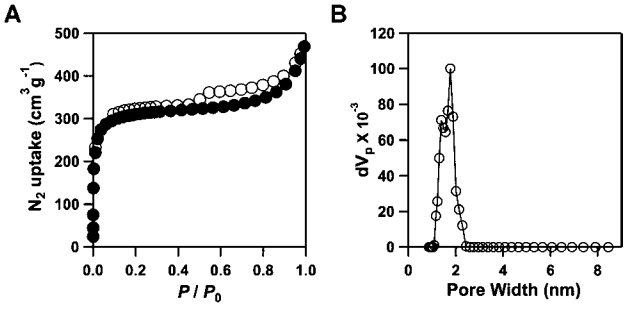

Figure 2. (A) N_2 adsorption (●) and desorption (○) isotherm curves and (B) pore size distribution profile of the Py-Azine COF.

up to 2.2 nm (Figure 2B), which is close to the theoretical pore size (1.96 nm). On the other hand, the imine-linked pyrene COF, ILCOF-1, is a mesoporous material with the pore size of 2.3 nm and BET surface area of 2723 $m^2\ g^{-1}$.[21]

To investigate the chemical stability of the azine-linked COF, we dispersed the COF samples in different organic solvents such as hexane, THF, MeOH, aqueous HCl (1 M) and NaOH (1 M) solutions at 25 °C for 24 h. We found that no decomposition occurs to the COF samples in these conditions. The samples were collected, washed with THF, dried under vacuum at 120 °C for 12 h, and subjected to XRD measurements. Surprisingly, all the samples exhibit intense XRD patterns, indicating that the high crystallinity is retained in the COF samples (Figure 3). Such a high chemical stability of COFs in different solvents is rare, which indicates that the azine linkage is chemically robust. The linear and conjugated azine

dx.doi.org/10.1021/ja4103293 | J. Am. Chem. Soc. 2013, 135, 17310–17313

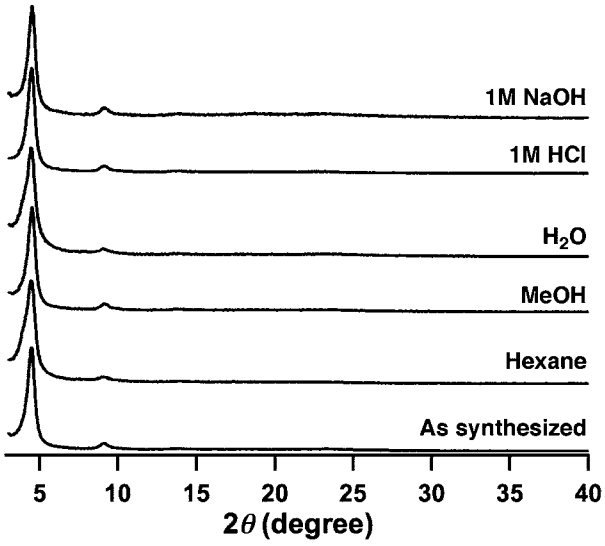

Figure 3. XRD patterns of the Py-Azine COF upon 1-day treatment in different conditions.

linkage may attribute to the high stability of the COF. The stable skeletons open up a new avenue for further applications of COF materials.

Electronic absorption spectrum of the Py-Azine COF dispersed in acetonitrile exhibited a broad absorption peak centered at 470 nm, which can be attributed to the $S_0 \rightarrow S_1$ transition (Figure S5A, red curve).[22] However, the TFPPy monomer exhibited the absorption band at 415 nm (black curve). This large redshift observed for the Py-Azine COF indicates that the azine bond links the vertices and edges in a fashion of π conjugation, which allows an extended π delocalization over the 2D skeleton. Upon excitation at 415 nm, the TFPPy monomer in acetonitrile emitted a bluish green fluorescence centered at 462 nm (Figure S5B). The Py-Azine COF emitted a yellow luminescence with a red-shifted band centered at 522 nm upon excitation at 470 nm.

The azine-linked pyrene COF offers a fluorescent channel and serves as a unique chemosensing detector.[23,24] We found that the azine units located at the edges provide open docking sites for forming hydrogen-bonding interactions with guest molecules.[20] This interaction likely manages the fluorescence quenching and gives rise to a selective detection of guests. We tested the chemosensing of a variety of nitrobenzene derivatives, including 2,4,6-trinitrophenol (TNP), 2,4-dinitrophenol (DNP), 2,4-dinitrotoluene (DNT), 2-nitrophenol (NP), and 2-nitrotoluene (NT), which are highly soluble in acetonitrile. Among these chemicals, TNP is designated as an explosive. When the solution of Py-Azine COF was exposed to the TNP vapor,[24a,25] the COF fluorescence was quickly quenched (Figure S6). The fluorescence quenching degree reaches 69% when the concentration of TNP is as low as 70 ppm in acetonitrile (Figure 4A), which indicates that the COF is highly sensitive to TNP molecules (Figure 4B). Surprisingly, when other nitrobenzene compounds were utilized under otherwise same condition, the COF did not show significant change. For example, the fluorescence quenching degrees are only 13%, 5%, 3%, and 3% for DNP, DNT, NP, and NT, respectively (Figure 4B, Figure S5C–F). These remarkable results indicate that the Py-Azine COF offers a selective detection of TNP explosive among the above nitrobenzene compounds. Such a selective detection remains a challenge for

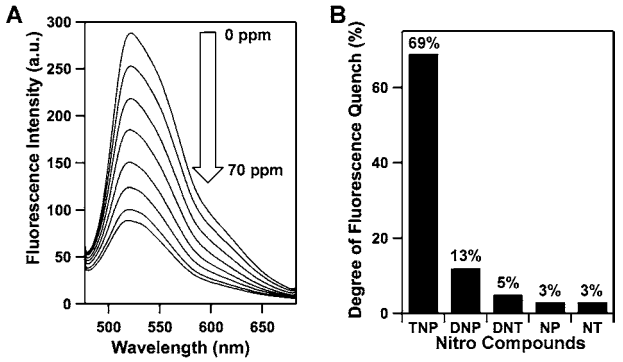

Figure 4. (A) Fluorescence quenching of the Py-Azine COF upon addition of TNP (0–70 ppm) in acetonitrile. (B) Degree of fluorescence quench upon addition of the nitro compounds (70 ppm).

chemosensors that usually work on static and dynamic quenching mechanisms.

To reveal the quenching mechanism of the present chemosensing system, the Stern–Volmer plot was employed to evaluate the quenching constant.[26] The Stern–Volmer quenching constant (k_{SV}) for TNP is estimated to be 7.8×10^4 M^{-1}, which is 37 and 86 times higher than those of DNP (2.1×10^3 M^{-1}) and DNT (9.1×10^2 M^{-1}), respectively (Figure S7, Table S2). A general tendency in quenching constant follows the order TNP ≫ DNP > DNT, NP, NT. An almost doubled quenching constant observed for DNP compared with DNT also suggests that the presence of phenol groups in the guest molecules is important, because the hydroxy units form hydrogen-bonding interactions with the open nitrogen atoms in the azine units on the pore walls.[20,27−29] Such a ground-state complexation facilitates the fluorescence quenching process. The functions of the nitro groups on the benzene ring are twofold; they affect the electron deficiency of the π system, and control the strength (acidity) of the phenol units for hydrogen-bonding interaction. In the case of TNP, three nitro groups result in the most deficient π system for driving the fluorescence quenching and the most strong interaction with the azine edges for promoting the quenching process. As a result, the Py-Azine COF exhibits an unusual sensitivity and selectivity in response to TNP.

Time-resolved fluorescence spectroscopy was conducted to probe the quenching dynamics. The Py-Azine COF in acetonitrile has an average lifetime (τ_0) of 0.8 ns. In the presence of TNP, the lifetime (τ) of the Py-Azine COF does not change, irrespective of the TNP concentration (Figure S8). Clearly, the unchanged lifetime is consistent with the ground-state complexation in the static fluorescence quenching reported in literatures.[27−30] The complexation of TNP with the Py-Azine COF forms nonemissive complex that traps the excitation energy of the COF skeletons. Indeed, fluorescence anisotropy measurement revealed that the exciton in the Py-Azine COF is not localized but migrate over the skeleton (Figure S9).[6] The exciton migration leads to a very high sensitivity. Considering all these results, together with the lifetime, the apparent quenching constant k_q ($k_q = k_{SV}/\tau_0$) for the Py-Azine COF/TNP system is evaluated to be 9.8×10^{13} M^{-1} s^{-1} (Table S2). This k_q value is even 3 orders of magnitude higher than that ($\sim 10^{10}$ M^{-1} S^{1-}) of conventional bimolecular quenching systems controlled by diffusion mechanism.[30,31] The above mechanistic insights demonstrate that the Py-Azine COF offers a platform as a unique chemosensing device, whereas the

dx.doi.org/10.1021/ja4103293 | J. Am. Chem. Soc. 2013, 135, 17310−17313

pyrene vertices, azine edges, and π-conjugated skeleton synergistically work to achieve the high sensitivity and selectivity.

In summary, we have explored a new covalent bond based on the azine linkage for the formation of covalent organic frameworks. The azine linkage endows the COFs with high crystallinity, high porosity, and robust chemical stability. We demonstrate that the integration of C_2 geometric pyrene units as building blocks for the vertices leads to the generation of luminescent, microporous, rhombic-shaped 2D COFs. By virtue of the synergistic functions of the pyrene vertices as luminescence emitter, the azine edges as docking sites for hydrogen-bonding interactions, and the extended π conjugation network as a media for exciton migration, the resulting COF features unique chemosensing device with high sensitivity and selectivity in detecting trinitrophenol type explosive, showing for the first time the utility of COFs for developing chemosensing systems. Considering the broad diversity of aldehyde derivatives together with the effectiveness of various solvents for the synthesis of the azine COF as shown by the present case, the azine linkage could be widely extended to other aldehydes, which allow not only structural predesign but also functional exploration based on the robust frameworks. Therefore, the present study constitutes an important step to the further advancement of the field of COFs.

■ ASSOCIATED CONTENT

Supporting Information

Materials and methods, syntheses and characterizations, Tables S1, S2, and Figures S1−S9. This material is available free of charge via the Internet at http://pubs.acs.org.

■ AUTHOR INFORMATION

Corresponding Author

jiang@ims.ac.jp

Notes

The authors declare no competing financial interest.

■ ACKNOWLEDGMENTS

S.D. would like to acknowledge IMS for fellowship grant. This work was supported by a Grant-in-Aid for Scientific Research (A) (24245030) from the Ministry of Education, Culture, Sports, Science and Technology, Japan (MEXT) and NSFC (Grant No. 21128001).

■ REFERENCES

(1) Feng, X.; Ding, X.; Jiang, D. *Chem. Soc. Rev.* **2012**, *41*, 6010−6022.

(2) Côté, A. P.; Benin, A. I.; Ockwig, N. W.; Matzger, A. J.; O'Keeffe, M.; Yaghi, O. M. *Science* **2005**, *310*, 1166−1170.

(3) El-Kaderi, H. M.; Hunt, J. R.; Mendoza-Cortes, J. L.; Côté, A. P.; Taylor, R. E.; O'Keeffe, M.; Yaghi, O. M. *Science* **2007**, *316*, 268−272.

(4) Côté, A. P.; El-Kaderi, H. M.; Furukawa, H.; Hunt, J. R.; Yaghi, O. M. *J. Am. Chem. Soc.* **2007**, *129*, 12914−12915.

(5) Tilford, R. W.; Gemmil, W. R.; zur Loye, H.-C.; Lavigne, J. J. *Chem. Mater.* **2006**, *18*, 5296−5301.

(6) Wan, S.; Guo, J.; Kim, J.; Ihee, H.; Jian, D. *Angew. Chem., Int. Ed.* **2008**, *47*, 8826−8830.

(7) Tilford, R. W.; Mugavero, S. J., III; Pellechia, P. J.; Lavigne, J. J. *Adv. Mater.* **2008**, *20*, 2741−2746.

(8) (a) Spitler, E. L.; Dichtel, W. R. *Nat. Chem.* **2010**, *2*, 672−677. (b) Colson, J. W.; Woll, A. R.; Mukherjee, A.; Levendorf, M. P.; Spitler, E. L.; Shields, V. B.; Spencer, M. G.; Park, J.; Dichtel, W. R. *Science* **2011**, *332*, 228−231. (c) Spitler, E. L.; Giovino, M. R.; White, S. L.; Dichtel, W. R. *Chem. Sci.* **2011**, *2*, 1588−1593. (d) Spitler, E. L.; Koo, B. T.; Novotney, J. L.; Colson, J. W.; Uribe-Romo, F. J.; Gutierrez, G. D.; Clancy, P.; Dichtel, W. R. *J. Am. Chem. Soc.* **2011**, *133*, 19416−19421. (e) Bunck, D. N.; Dichtel, W. R. *Angew. Chem., Int. Ed.* **2012**, *51*, 1885−1889. (f) Spitler, E. L.; Colson, J. W.; Uribe-Romo, F. J.; Woll, A. R.; Giovino, M. R.; Saldivar, A.; Dichtel, W. R. *Angew. Chem., Int. Ed.* **2012**, *51*, 2623−2627.

(9) Dogru, M.; Sonnauer, A.; Gavryushin, A.; Knochel, P.; Bein, T. *Chem. Commun.* **2011**, *47*, 1707−1709.

(10) Ding, X.; Guo, J.; Feng, X.; Honsho, Y.; Guo, J.; Seki, S.; Maitarad, P.; Saeki, A.; Nagase, S.; Jiang, D. *Angew. Chem., Int. Ed.* **2011**, *50*, 1289−1293.

(11) Wan, S.; Guo, J.; Kim, J.; Ihee, H.; Jiang, D. L. *Angew. Chem., Int. Ed.* **2009**, *48*, 5439−5442.

(12) Hunt, J. R.; Doonan, C. J.; LeVangie, J. D.; Côté, A. P.; Yaghi, O. M. *J. Am. Chem. Soc.* **2008**, *130*, 11872−11873.

(13) Uribe-Romo, F. J.; Hunt, J. R.; Furukawa, H.; Klöck, C.; O'Keeffe, M.; Yaghi, O. M. *J. Am. Chem. Soc.* **2009**, *131*, 4570−4571.

(14) Chen, X.; Addicoat, M.; Irle, S.; Nagai, A.; Jiang, D. *J. Am. Chem. Soc.* **2013**, *135*, 546−549.

(15) Kuhn, P.; Antonietti, M.; Thomas, A. *Angew. Chem., Int. Ed.* **2008**, *47*, 3450−3453.

(16) Uribe-Romo, F. J.; Doonan, C. J.; Furukawa, H.; Oisaki, K.; Yaghi, O. M. *J. Am. Chem. Soc.* **2011**, *133*, 11478−11481.

(17) Nagai, A.; Chen, X.; Feng, X.; Ding, X.; Guo, Z.; Jiang, D. *Angew. Chem., Int. Ed.* **2013**, *52*, 3770−3774.

(18) Jackson, K. T.; Reich, T. E.; El-Kaderi, H. M. *Chem. Commun.* **2012**, *48*, 8823−8825.

(19) Kandambeth, S.; Mallick, A.; Lukose, B.; Mane, M. V.; Heine, T.; Banerjee, R. *J. Am. Chem. Soc.* **2012**, *134*, 19524−19527.

(20) Ray, D.; Dalapati, S.; Guchhait, N. *Spectrochim. Acta, Part A* **2013**, *115*, 219−226.

(21) Rabbani, M. G.; Sekizkardes, A. K.; Kahveci, Z.; Reich, T. E.; Ding, R.; El-Kaderi, H. M. *Chem.—Eur. J.* **2013**, *19*, 3324−3328.

(22) Jana, S.; Dalapati, S.; Guchhait, N. *J. Phys. Chem. A* **2012**, *116*, 10948−10958.

(23) (a) Peng, Y.; Zhang, A.-J.; Dong, M.; Wang, Y.-W. *Chem. Commun.* **2011**, *47*, 4505−4507. (b) Rochat, S.; Swager, T. M. *ACS Appl. Mater. Interfaces* **2013**, *5*, 4488−4502. (c) Toal, S. J.; Trogler, W. C. *J. Mater. Chem.* **2006**, *16*, 2871−2883.

(24) (a) Vij, V.; Bhalla, V.; Kumar, M. *ACS Appl. Mater. Interfaces* **2013**, *5*, 5373−5380. (b) Ma, Y.; Li, H.; Peng, S.; Wang, L. *Anal. Chem.* **2012**, *84*, 8415−8421. (c) Salinas, Y.; Martínez-Máñez, R.; Marcos, M. D.; Sancenón, F.; Costero, A. M.; Gil, M. P. S. *Chem. Soc. Rev.* **2012**, *41*, 1261−1296.

(25) Deng, C.; He, Q.; He, C.; Shi, L.; Cheng, J.; Lin, T. *J. Phys. Chem. B* **2010**, *114*, 4725−4730.

(26) Ganguly, A.; Paul, B. K.; Ghosh, S.; Kar, S.; Guchhait, N. *Analyst* **2013**, *138*, 6532−6541.

(27) Gole, B.; Shanmugaraju, S.; Bar, A. K.; Mukherjee, P. S. *Chem. Commun.* **2011**, *47*, 10046−10048.

(28) Kim, T. K.; Lee, J. H.; Moon, D.; Moon, H. R. *Inorg. Chem.* **2013**, *52*, 589−595.

(29) Sohn, H.; Sailor, M. J.; Magde, D.; Trogler, W. C. *J. Am. Chem. Soc.* **2003**, *125*, 3821−3830.

(30) Manman, Y.; Xiaoli, X.; Pin, Y. *Chin. Sci. Bull.* **2005**, *50*, 2571−2574.

(31) Olley, D. A.; Wren, E. J.; Vamvounis, G.; Fernee, M. J.; Wang, X.; Burn, P. L.; Meredith, P.; Shaw, P. E. *Chem. Mater.* **2011**, *23*, 789−794.